applied sciences

MDPI

Article

Study on Temporal and Spatial Distribution of Landslides in the Upper Reaches of the Yellow River

Zongren Li [1,2,3], Sailajia Wei [4,*], Kai Wu [5], Yonglian Sha [1,2,3], Xing Zhang [1,2,3], Delin Li [1,2,3], Rongfang Xin [1,2,3] and Peng Guan [6]

1 Institute of Geological Survey of Qinghai Province, Xining 810000, China
2 Qinghai Remote Sensing Big Data Engineering Technology Research Center, Xining 810012, China
3 The Northern Qinghai-Tibet Plateau Geological Processes and Mineral Resources Laboratory, Qinghai Geological Survey Institute, Xining 810000, China
4 Geological Environment Monitoring Station of Qinghai Provincial, Xining 810000, China
5 Hubei Shenlong Geological Engineering Investigation Institute Co., Ltd., Wuhan 430000, China
6 Faculty of Engineering, China University of Geosciences, Wuhan 430000, China
* Correspondence: weisai1212@163.com

Abstract: The geological structure of the upper reaches of the Yellow River is complex, especially in the Sigouxia-Laganxia section. It has always been a high-incidence area of landslide disasters, which poses a threat to the safe operation of the upper reaches of the Yellow River. In this study, based on the high-precision remote sensing image data, the spatial distribution of each landslide was obtained by superimposing the remote sensing image and the 1:50,000 digital elevation model (DEM). Some typical landslides were selected for detailed field investigation and field verification. The results show that the remote sensing image characteristics of landslides in the upper reaches of the Yellow River are obvious. Through remote sensing interpretation and field investigation, a total of 508 landslides of various types were found, including 24 giant landslides. The spatial spreading patterns of landslides mainly include six types: dumb-bell shape, rectangle, saddle type, long arc shape, triangle, and side-by-side shape. The length and width of the landslide deposit are mainly concentrated at 550–1500 m and 600–1500 m, and the average elevation of the sliding body is mainly concentrated between 2000 and 2800 m. The average slope of the landslide is mainly distributed between 15–20°. Giant landslides are mainly distributed in the Jianzha basin area, surrounded by the Jishishan fault and the Lajishan fault in the West Qinling Mountains. The spatial distribution characteristics of giant landslides have obvious regional differences due to different factors such as lithologic differences and riverside erosion. The research results are of great significance for the early identification, prevention, and mitigation of landslide disasters in the upper reaches of the Yellow River.

Keywords: landslide; the upper reaches of the Yellow River; remote sensing interpretation; spatial and temporal distribution; disaster prevention and mitigation

Citation: Li, Z.; Wei, S.; Wu, K.; Sha, Y.; Zhang, X.; Li, D.; Xin, R.; Guan, P. Study on Temporal and Spatial Distribution of Landslides in the Upper Reaches of the Yellow River. *Appl. Sci.* **2024**, *14*, 5488. https://doi.org/10.3390/app14135488

Academic Editor: Tiago Miranda

Received: 15 May 2024
Revised: 12 June 2024
Accepted: 20 June 2024
Published: 25 June 2024

1. Introduction

In recent years, due to the influence of global extreme climate events, the frequency of landslide disasters, especially large-scale and extra-large landslide disasters, has become higher and higher [1]. A landslide is a typical mode of surface slope failure and a manifestation of the geomorphological evolution process. It is formed, developed, and evolved under the combined action of geological internal dynamics such as active structure and external dynamic conditions such as climate change [2]. The formation, development, and evolution of landslides are directly or indirectly affected by internal dynamic effects such as crustal uplift [3], fault activity [4], and earthquake [5]. Climate change will have an important impact on topography, hydrological conditions, and river erosion and often trigger the occurrence of landslides [6,7].

Different experts and scholars have studied the evolution process of landslides by means of landslide spatial form, mutual superposition relationships, and terrace chronology in river valley areas [8–12]. Among them, Journault et al. [8] analyzed the geological history of the Thompson Valley, then monitored the deformation rate of the landslide using the InSAR measurements and found that most Thompson Valley land-slides exhibit seasonal changes in displacement rate. Li et al. [9] analyzed the formation mechanism of the reservoir bank landslide with stepped sliding surfaces in the Three Gorges Reservoir area, established a representative geological model with multiple stepped sliding surfaces, and believed that the formation of the stepped landslide surface was closely related to the Jurassic strata with interlayers and weak hard layers. Regmi [10] studied the development characteristics of landslides, such as landslide area and landslide volume, through aerial photography and field investigation and established a conceptual model of river cutting, shallow landslides and deep large land-slides driving downslope facing highlands and plateaus. Chen et al. [11] analyzed the geological process of landslide development and river evolution in the Three Gorges Reservoir area of the Yangtze River. Yin et al. [12] studied the response process of landslide development in the upper reaches of the Yellow River to plateau uplift and river incision.

Regarding the response relationship between landslide development and geo-morphological evolution in the study area, Su et al. [13] believed that there may be a relationship between the formation of terraces and the glacial-interglacial climate cycle. The differences in the sequence and age of the Yellow River terraces in the western Henan fault uplift zone and the Huaibei fault depression zone indicate that surface uplift played an important role in the formation of these terraces. Li et al. [14] studied the geomorphological evolution of the upper reaches of the Yellow River and the uplift process of the Qinghai-Tibet Plateau in the late Cenozoic. This series of plateau uplifts and the Yellow River incised background provide broad space conditions and material sources for the development of landslides in the study area. Based on the measurement and dating of the river terraces, Liu [15] drew the profile of the typical river terraces and analyzed the neotectonic movement of the river terraces in detail. Each tectonic movement developed large-scale geological disasters such as landslides and de-bris flows, and the geological disaster effect was very obvious.

At present, research on the spatial and temporal distribution of landslides mainly focuses on the distribution law and inducing factors of landslides in space and time by field investigation, remote sensing interpretation, and dating [16]. Guo et al. [17] collected OSL samples from the sediment covering the landslide and analyzed the absolute age of the landslide. The study suggests that the formation of the Dehenglong landslide is closely related to tectonic activity. Li et al. [18] believed that China's land-slide disasters are mainly distributed in six areas: the high and middle mountains in southwestern Yunnan, the high and middle mountains in southwestern Sichuan, the Loess Plateau in central Gansu and eastern Gansu, the Taihang Mountains in Lyuliang Mountains, the high and middle mountains in Daba Mountains in Qinling Mountains, and the mountainous areas in central Hubei, Guizhou and Yunnan. On the basis of a field investigation, Gariano et al. [19] believe global warming is expected to increase the frequency and intensity of severe rainfall events, a primary trigger of rapid-moving landslides that cause many landslide fatalities. Chigira [20] believed that strong earthquakes, extreme weather and climate events, and global climate change events were also the main triggers and inducing factors of landslides.

There are many studies on landslide dynamics and landslide disaster science, such as the characteristics and genetic mechanisms of the sliding body of a single landslide. However, there are few studies on the regional distribution of landslides in the Upper Reaches of the Yellow River. In fact, the geological structure of the upper reaches of the Yellow River is complex, especially in the Sigouxia-Laganxia section. Therefore, the study of the regional distribution of landslides can help understand the development process, influence range, and trigger factors of landslides, which will provide enlightenment for the study of landslide disasters.

2. Topographic Features of the Upper Reaches of the Yellow River

The upper reaches of the Yellow River are located on the northeastern margin of the Qinghai-Tibet Plateau (Figure 1). It starts from the Lagan Gorge at the southeastern end of the Gonghe Basin in the west and reaches the Sigou Gorge at the eastern end of the Guanting Basin in the east. The Yellow River passes through the Gonghe Basin, Guide Basin, Qunke-Jianzha Basin, Xinhua Basin and Guanting Basin from upstream to downstream.

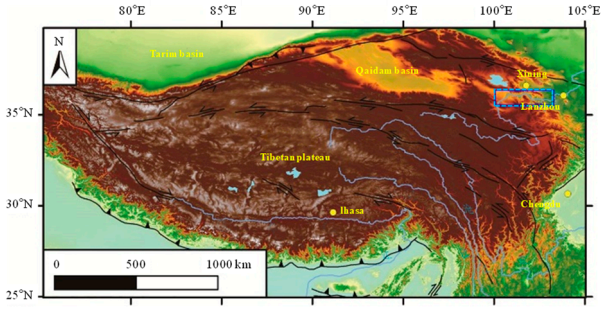

Figure 1. The location of the upper reaches of the Yellow River in the Qinghai-Tibet Plateau.

There are five intermountain basins in the study area, including Gonghe, Guide, Qunke-Jianzha, Xunhua and Guanting (Figure 2). Each basin is separated by mountains. For example, Gonghe Basin and Guide Basin are separated by Nanshan of Qing-hai Lake and Waligong Mountain. Guide Basin and Qunke-Jianzha Basin are separated by Zama Zari Mountain. Qunke-Jianzha Basin and Xunhua Basin are separated by Jishi Mountain. Xunhua Basin and Guanting Basin are separated by Laji Mountain. From bottom to top, the canyons are Jishixia, Gongboxia, Lijiaxia, Songbaxia and Longyang-xia. Under the dual effects of internal and external geological forces, many high-steep rock-soil slopes with a height of 200–900 m have been intermittently shaped along both sides of the river. The extensive development of these high-steep slopes has provided favorable topographic conditions for the large-scale development of landslides in the study area. The quaternary strata and lithology in the study area, as shown in Table 1.

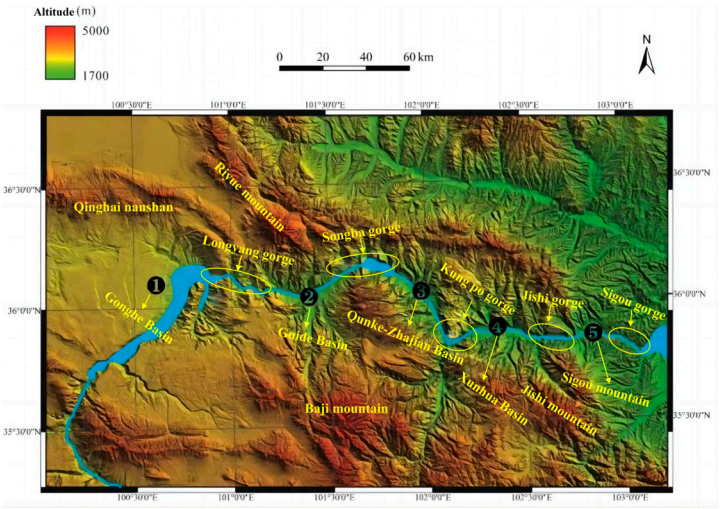

Figure 2. Topographical map of basin and mountain in the upper reaches of the Yellow River.

Table 1. Quaternary strata and lithology in the study area.

System	Series	Sign	Sedimentary Facies and Material Composition
Quaternary	Holocene	Q_4^{eol}	Wind phase It is composed of beige medium and fine quartz sand (more than 80%) and a small amount of dark minerals. The gravel is round and the particle size is generally greater than 0.5 mm. The thickness is generally 20–40 m.
		Q_4^{pl}	Pluvial phase The lithology is mainly breccia, gravel and sand, with sub-sand lens. The sorting and roundness are poor, and the thickness is 12–30 m.
		Q_4^{al-pl}	Alluvial-diluvial facies The lithology is gray and soil gray sand gravel layer with sand lens, and the upper part is fine sand. The structure is loose and the thick-ness changes greatly, generally 10–30 m.
		Q_4^{al}	Alluvial phase It is mainly composed of riverbed sand gravel pebble layer and floodplain silty sand, fine sand, sandy soil, clay and so on. Gravel sorting, roundness is better, generally 5–10 cm. The thickness is generally 10–20 m.
	Epipleistocene	Q_3^{eol}	Wind phase Earthy yellow, light grayish yellow silt. The silt content is more than 70%, with macropores and vertical joints. The thickness is 50–260 m.
		Q_3^{al-pl}	Alluvial-diluvial facies Gray gravel, sand and sub-clay layers. The sorting and roundness are poor, the gravel composition varies from place to place, and the thickness is generally greater than 30 m.
		Q_3^{pl}	Pluvial phase The gray-soil gray sand-gravel layer is sandwiched with gravel-sand lens. The gravel composition is complex, mostly angular, sub-angular, muddy and sandy filling, 30–60 m thick, medium density. The thickness is generally greater than 30 m.
		Q_3^{al}	Alluvial phase It is composed of a set of alluvial facies, the lower part is gravel layer, and the upper part is fine sand and silt, loess, loess-like clay layer, with a thickness of 5–30 m.
	Middle Pleistocene	Q_2^{fgl}	Ice-water phase accumulation The lithology is gray-yellow sandstone, slate, granite, etc., which are poorly sorted and rounded. The mud gravel and sand gravel layer composed of gravel and sand, with a layer of yellow sandy soil, 5–15 m thick.
	Lower Pleistocene	Q_1	The Gonghe Basin is a set of yellow and grayish yellow silty mud-stone, siltstone mixed with colored fine sandstone and sand-containing gravel lens. The area of Yezangcaotan and Yelangtan in Guide Basin is a set of conglomerate and fine siltstone with sandstone, which is generally exposed at an altitude of 2800–3300 m. Leyangsang in Hualong Basin is a set of gray-white-light orange-yellow conglomerate, glutenite with thin sandstone and mudstone. The thickness is 206–405 m.

3. Temporal and Spatial Distribution of Landslides in the Upper Reaches of the Yellow River

3.1. Material and Methods

The process of remote sensing interpretation and recognition of regional landslide disasters mainly includes five parts: image preprocessing, establishment of interpretation

marks, image segmentation, image classification, and accuracy evaluation. The image preprocessing of this study is carried out in the environment for visualizing images (ENVI) 5.3 software, and the image segmentation, classification, and accuracy evaluation are completed in the e-Cogniton 9.0 software. The specific process of remote sensing interpretation and identification of landslide disasters in the study area is shown in Figure 3.

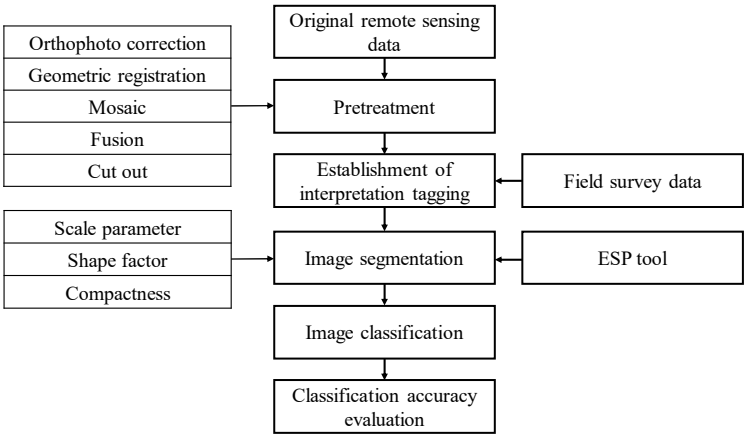

Figure 3. Remote sensing identification process of landslide disasters in the study area.

During remote sensing imaging, various factors lead to certain phenomena, such as geometric deformation and radiation changes in remote sensing images, which are unfavorable for the analysis of remote sensing images. Therefore, the preprocessing of remote sensing images is a crucial step before conducting image analysis. The process of image preprocessing mainly includes orthorectification, geometric registration, image mosaicking, image fusion, and image clipping. Since the study area is a high and steep canyon region that exceeds the coverage of a single remote sensing image, the precision requirement for image preprocessing is very high. We utilize professional remote sensing software ENVI and auxiliary digital elevation model (DEM) data to preprocess the images and obtain the experimental images.

The remote sensing identification of landslides is a technical method that utilizes remote sensing images, combined with human–computer interaction and visual interpretation, to obtain relevant information about landslides. Its principle is based on the differences in tone, shape, shadow, texture, and pattern between landslide bodies and their background geological bodies. These differences manifest as specific combinations of tone, texture, and geometric shapes on remote sensing images, known as direct interpretation signs for landslide identification [21].

Based on field investigation data, representative landslides in the study area were selected for establishing the interpretation markers. Subsequently, the remote sensing characteristics of landslides in high and steep canyon areas were summarized based on remote sensing images.

By comparing the field investigation data, typical landslides were selected to analyze their development characteristics. Most of the landslides are water-related and are distributed along both banks of the river. Ultimately, the landslide disaster interpretation markers in the study area were determined to have spectral features and shape characteristics. Spectral features are primarily manifested as: relatively developed vegetation on the surface of the landslide body, with scattered small collapses; and the base of the landslide is the reservoir bank slope. The shape characteristics of the land-slide development can be observed through the distinct gullies on both sides of the landslide, mainly manifesting as rectangle, triangle, side-by-side shape, and so on.

Landslides are represented as individual image objects on remote sensing images, and their classification utilizes the spectral and geometric characteristics of these objects. Therefore, the interpretation of landslides in remote sensing adopts the object-oriented

image classification approach. Object-oriented image classification mainly consists of two parts: image object construction and object classification.

The construction of landslide images utilizes the multi-scale segmentation algorithm in e-Cognition software to perform segmentation experiments on the images of the study area. Before conducting the segmentation experiments, the band combination of the images can be performed, which can comprehensively select the characteristics of each band to improve the interpretability of ground features and make the interpretation results more scientific and reasonable [22]. In multiscale segmentation algorithms, it is necessary to consider two factors that affect image heterogeneity: the spectral factor and the shape factor, which in turn include smoothness heterogeneity and compactness heterogeneity. Due to the time-consuming nature of multi-scale segmentation algorithms, representative areas of landslides in the study area were selected. Meanwhile, in order to determine the optimal segmentation scale while ensuring high homogeneity of landslide objects. Using Estimation of Scale Parameter (ESP) as a scale evaluation tool [23,24]. This tool calculates the local variation (LV) of image object homogeneity under different segmentation scale parameters as the standard deviation of the segmentation object layer in order to determine whether the segmentation effect is optimal. Use the rate of change value ROC-LV (rates of change in LV) to indicate the optimal scale parameter for object segmentation. When the rate of change reaches its maximum and reaches its peak, the segmentation scale value corresponding to that point is the optimal segmentation scale. Select the optimal segmentation scale parameter for land features by visually judging the segmentation effect and matching it with the vector image.

3.2. Spatial Geometric Distribution Characteristics of Landslide

Using high-resolution satellite remote sensing images (Table 2), it is found that there are 508 landslides of various types in the Sigouxia-Laganxia section of the upper reaches of the Yellow River. The remote sensing image and the 1:50,000 digital elevation model are superimposed to obtain the spatial distribution pattern of each landslide, the length and width of the landslide accumulation body, the elevation value of the front and rear edges, the slope value of the landslide accumulation body, and the slope direction. Based on the field investigation, the author obtained the thickness information for 116 landslides. On the basis of remote sensing interpretation, we selected some typical landslides for detailed field investigation and field verification. The landslide distribution map of the study area is shown in Figure 4.

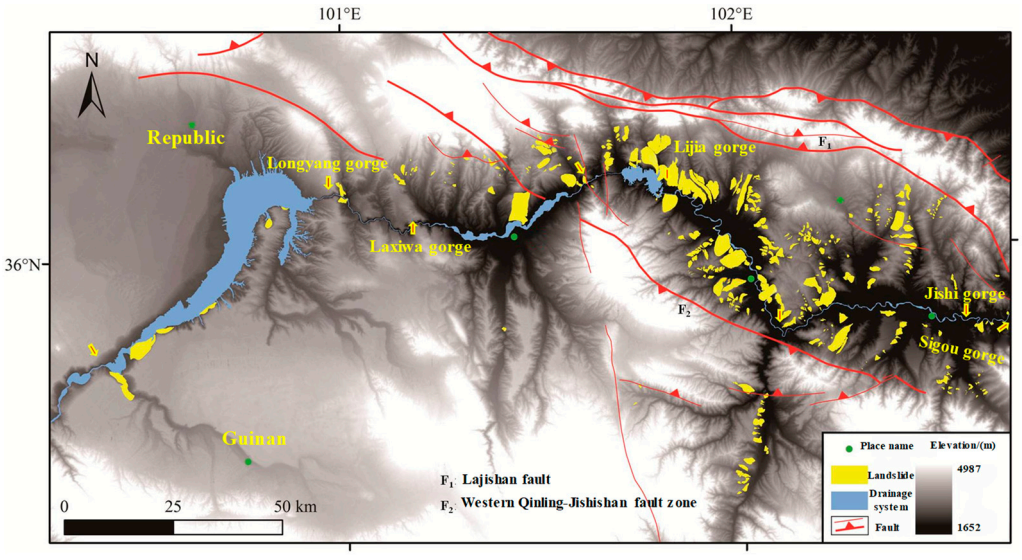

Figure 4. Landslide distribution map of the study area.

Table 2. Satellite data characteristics used in landslide remote sensing image interpretation.

Data Type	Spectral Characteristics	Spatial Resolution	Receiving Time	Main Uses
QuickBird	4 bands from visible to near-infrared, 1 band of full color	Panchromatic image 0.61 m, multispectral image 2.4 m	August 2006	Landslide information extraction in disaster area
GeoEye	Multi-spectral blue, green, red and near infrared four bands, panchromatic one band	Panchromatic image 0.41 m, multispectral image 1.65 m	May 2007, September 2009, March 2012	Macro information extraction of landslide development
ZY-3	Multispectral 4 bands, panchromatic 1 band	Panchromatic image 2.1 m, multispectral image 6 m	May 2012	Natural disaster prevention, environmental monitoring and protection
ZY-1 02C	Multispectral 3 bands, panchromatic 1 band	Panchromatic image 2.36 m, multispectral image 10 m	April 2012	Geological disaster investigation, monitoring, etc.

The morphological characteristics of landslides in the study area are very obvious; the plane shape of the trailing edge of the landslide presents a typical ring chair shape, and the back wall is generally steep, with a slope of 15–25°. The front edge of the landslide is tongue-shaped or long tongue-shaped. The front edge of the ancient landslide and the old landslide have been eroded many times, and even most or all of the sliding body has been eroded clean. Only the chair-shaped shape of the trailing edge and a small amount of steep slope remaining due to erosion are preserved. A high floodplain or terrace can be seen at the foot of the old landslide slope.

According to the characteristics of its spatial distribution (Google Earth), this study divides it into six types: dumb-bell shape, rectangle, saddle type, long arc shape, triangle, and side-by-side shape. The spatial form and detailed information of the representative landslide remote sensing images of each type of landslide are shown in Figure 5 and Table 3.

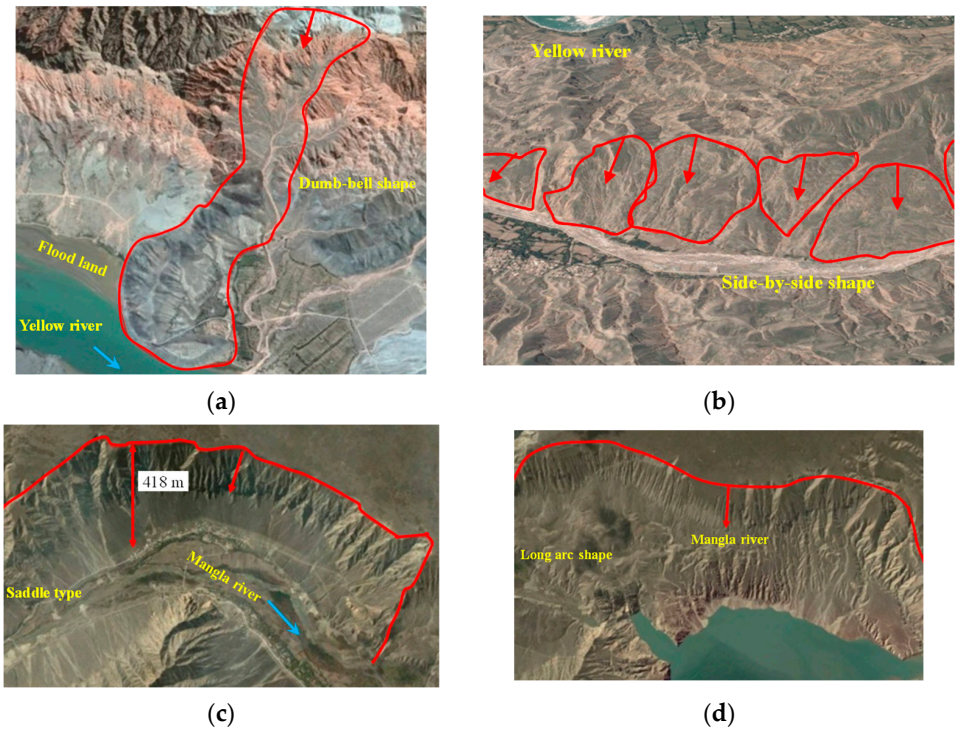

Figure 5. *Cont.*

(**e**) (**f**)

Figure 5. Plane morphological characteristics of landslide in the study area. (**a**) Dumb-bell shape; (**b**) Side-by-side shape; (**c**) Saddle type; (**d**) Long arc shape; (**e**) Triangle; (**f**) Rectangle.

Table 3. Representative landslide locations and image types.

Number	Plane Configuration	Representative Landslide	Latitude and Longitude Coordinates	Remote Sensing Image Type	Plane Morphological Characteristics
a	Dumb-bell shape	Kuogeza landslide	101°36′ E, 36°08′ N	Google earth GeoEye	Slide length is greater than width
b	Side-by-side shape	Zhaji ‘ang land-slide group	101°55′ E, 36°06′ N	ZY-3	Multiple single landslides are arranged side by side
c	Saddle type	Mangla River estuary landslide	100°27′ E, 35°42′ N	GeoEye-2	Trailing edge center bend
d	Long arc shape	Mangla River left bank landslide	100°26′ E, 35°43′ N	Google earth GeoEye	Lateral margins and pos-terior wall are curved
e	Triangle shape	Gelongbu landslide	102°36′ E, 49°12′ N	Google earth GeoEye	Regular triangle or in-verted triangle
f	Rectangle	Xijitan landslide	101°26′ E, 36°06′ N	ZY-3	Rectangular in shape with an upright back wall

According to the interpretation of remote sensing images, the author counted the length, width, slope, area, and volume of 508 landslides. Based on the statistical division of the above data, the main distribution areas and the most concentrated distribution areas of the length, width, thickness, area, and volume of each landslide were obtained. The length of the landslide in the study area spans a large range, with a minimum length of 120 m and a maximum length of 6500 m, mostly between 500 and 2200 m. Mainly concentrated in the 550–1500 m, there are 388, accounting for 76.4% of the total number of landslides; especially in the length of 550–1000 m landslides have 165, accounting for 32.5% (Table 4). The width of the landslide is also large, the minimum width is 90 m, the maximum is 7200 m, mostly 560–2500 m, mainly concentrated at 600–1500 m, there are 405, accounting for 79.7% of the total number of landslides (Table 5).

Table 4. Statistical table of landslide length.

Length Range/m	Number	Percentage of Total/%
≤550	111	21.9
551–970	165	32.5
971–1400	113	22.2
1401–2670	92	18.1
2671–4800	22	4.3
>4801	5	1.0

Table 5. Statistics of landslide width.

Width Range/m	Number	Percentage of Total/%
≤560	175	34.5
561–1040	144	28.3
1041–1510	89	17.5
1501–2930	71	14.1
2931–5300	23	4.5
>5300	6	1.1

Statistics show that there are a large number of landslides with a length greater than the width of the sliding body, which are mainly distributed on both sides of the mainstream of the Yellow River in the Qunke-Jianzha Basin. These slopes have large height differences and open free surfaces, so it is easy to form large-length landslides, such as Xiazangtan landslide, Kangyang landslide, Lannitan landslide, Shenguotan landslide, Sozi landslide, etc., which belong to the category of giant landslides in terms of volume, belong to mudstone landslides in terms of material composition type, and are mainly in the form of ring chairs, long tongues, giants, dumbbells, etc. This type of landslide has a long sliding distance and a large sliding speed, which is a typical high-speed and long-distance landslide type [25]. The Yellow River is partially blocked, forming a huge barrier lake, leaving landslide deposits on the other side of the Yellow River, such as the Suozi landslide and the Gelongbu landslide; some landslides belong to the creep type, with a short sliding distance and a small sliding speed, such as the Shangen landslide in Gongboxiakou. Meanwhile, landslides with width greater than length are mainly distributed in the Gonghe Basin on both sides of the main stream of the Yellow River, such as the Baicitan landslide, the Mangla River left bank landslide, and the Mangla River estuary landslide. The Yellow River tributary is generally narrow, the free surface is limited, and the wide body landslide is developed. From the material composition type, it belongs to the semi-consolidated diagenetic landslide, and the plane shape is mainly presented as semi-elliptical, dustpan-shaped, saddle-shaped, semi-arc-shaped, etc. The sliding distance of this type of landslide is short, and the back wall is well-preserved and has a straight and steep shape. Therefore, these two types of landslides are obviously different from each other in terms of sliding body morphology and material composition.

Among the 508 landslides in the study area, there are 303 landslides with a length greater than their width. There is a certain relationship between the length (L) and the width (W) of the landslide body. When the length and width of the landslide body are less than 1500 m, the ratio of width to length is close to 1, and this kind of landslide accounts for more than 1/5 in the study area. However, when it is greater than 1500 m, the length and width show a linear relationship, extending in the direction of polarization, but the overall increase in length is greater than the increase in width. The length-width ratio peaks at 2 and 3.2, reflecting that the length of some landslides is 2 times, 3 times, or even more than the width (Figure 6a). When it is greater than 1500 m, the length and width show a linear relationship, extending in the direction of polarization, but the overall increase in length is greater than the increase in width. As shown in the following figure, the correlation coefficients between length and width are 0.87 and 0.76, respectively (Figure 6b).

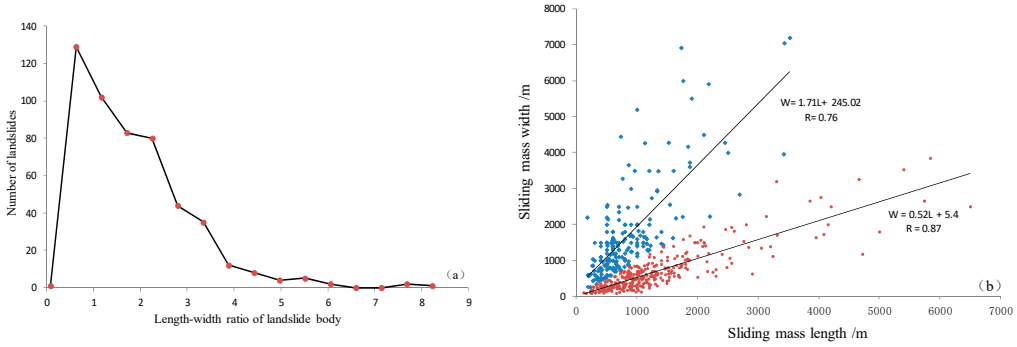

(**a**) (**b**)

Figure 6. Relationship between length and width of landslide. (**a**) Length-width ratio of landslide body; (**b**) The correlation coefficients between length and width.

The minimum thickness of 116 field survey landslides in the study area is 15 m, the maximum is 135 m, and the average thickness is 39.6 m. According to the classification standard of the thickness of the landslide accumulation body [26], the author counted the thickness of 116 landslides in the field survey and found that the thickness of the landslide body was mainly concentrated in 30–50 m, which was a deep landslide, accounting for 67.2% of the total number of surveys. In addition, there are 25 ultra-deep landslides greater than 50 m, mainly giant landslides, accounting for 21.6% of the total number of investigations, as shown in Table 6.

Table 6. Statistical table of landslide thickness.

Category	Number	Average Thickness/m	Landslide Thickness Classification/m			
			Shallow Landslide	Mid-Level Landslide	Deep-Seated Landslide	Ultra-Deep Landslides
			<10	10–25	25–50	>50
Number of individuals	116	39.6	0	13	78	25
Percentage/%			0	11.2	67.2	21.6

Among the 508 landslides, the smallest area is 0.01 km^2, the largest is 16.26 km^2, mainly distributed in the range of 0.01–4 km^2, of which 319 landslides with an area of 0.8–1.5 km^2, accounting for the vast majority, mainly distributed in the small slopes of the Qunke-Jianzha Basin and the Hualong Basin on the north bank of the Yellow River. Generally, the height difference and the free surface are not large, and the stratigraphic lithology is dominated by loess landslides. The number of landslides with an area of more than 4 km^2 is small, mainly distributed on both sides of the mainstream of the Yellow River and some large tributaries. For example, the Xiazangtan landslide on the south bank of the Yellow River in the Qunke-Jianzha Basin is stage I, and the sliding body area is 14.12 km^2. The total residual volume of 116 landslides is 98.35 $\times$ 10^8 m^3, and the average volume is 0.85 $\times$ 10^8 m^3. The residual volume peaks are mainly concentrated in four intervals: 0.5–4 $\times$ 10^8 m^3, 6–8 $\times$ 10^8 m^3, 10–12 $\times$ 10^8 m^3 and 15–17 $\times$ 10^8 m^3. The former two sections and the latter two sections belong to the category of super-large landslides and giant landslides, especially the giant landslides with >15 $\times$ 10^8 m^3 are developed in the mudstone strata of the study area, such as the Xiazangtan landslide phase I on the right bank of the Yellow River in the Qunke-Jianzha Basin and the Xijitan landslide on the left bank of the Yellow River in the Guide Basin, which are not developed in other strata.

3.3. Slope Characteristics of Landslide Body

As shown in Figure 7, the average slope of the landslide deposits in the study area is small, and most of them belong to small-angle landslides. Statistics show that they are mainly concentrated between 15–40°, especially 15–20° and 35–40°. Field investigation found that most of the 15–20° landslides have been stabilized, and the possibility of overall sliding is very small. Another group of landslides between 35° and 40° is more unstable, and it is very likely to be revived under the action of heavy precipitation and continuous precipitation.

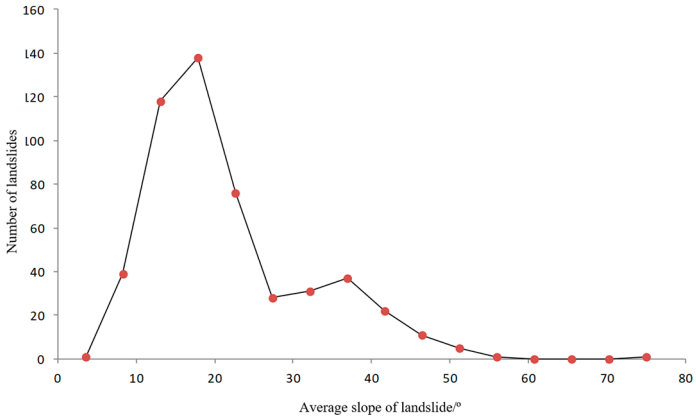

Figure 7. Landslide slope distribution map.

In addition, it was found that the length of the landslide body in the study area has a certain relationship with the slope. The longer the landslide body is, the smaller the average slope is. On a slope, if the sliding force of the slope is greater than its own friction, the slope is very unstable and prone to landslides under the action of inducing factors. Assuming that the sliding force of the slope is F, the friction force of the slope is f, the friction coefficient is μ, the component force of the gravity of the slope itself perpendicular to the slope is N, the slope has a gradient of α, the length of the slope is L, and the height difference between the front and rear edges is H, then there is:

$$\mu = \frac{f}{N} \tag{1}$$

$$\alpha = \frac{H}{L} \tag{2}$$

According to the similar triangle principle, there are:

$$\mu \propto \alpha \tag{3}$$

For the same slope body, its N is a fixed value, then:

$$\alpha \propto f \tag{4}$$

According to the principle of mechanics, when $F > f$, the slope will decline, and vice versa, it is stable. Therefore, when α is greater than a certain angle, the landslide will occur, and vice versa, it will be stable.

According to the above formula, it is deduced that the landslide with a large length has stabilized because of its small slope. For those landslides with smaller lengths, only a small number of them have stabilized. A large part of them are not stable because of their large sliding force, and their leading edge may be reactivated and disintegrated again; therefore, those landslides are above the fitting line, as shown in Figure 8.

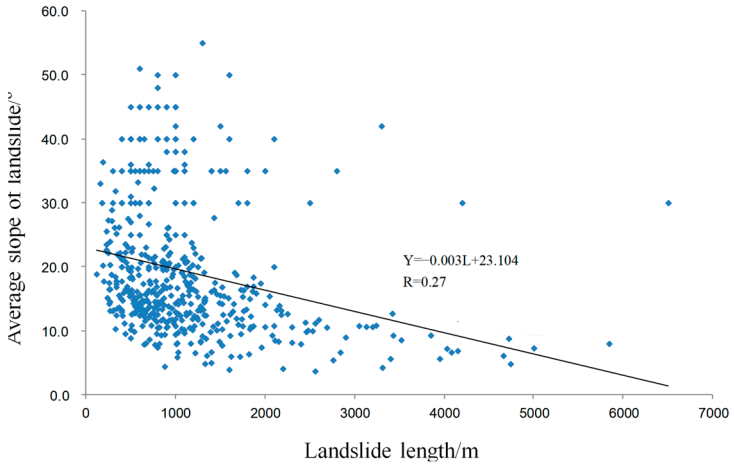

Figure 8. Relationship between landslide length and average slope.

4. Spatial Distribution Characteristics of Giant Landslides in the Upper Reaches of the Yellow River

Among the 508 landslides, they were classified according to the square amount of landslide deposits [26]. Super-large-scale landslides (with a square amount of landslide greater than 1×10^8 m^3) accounted for 21 of them (Figure 9, Table 7). Large-scale land-slides (accumulation volume greater than 1×10^7 m^3) accounted for 92 cases, and the rest were large-scale landslides or below.

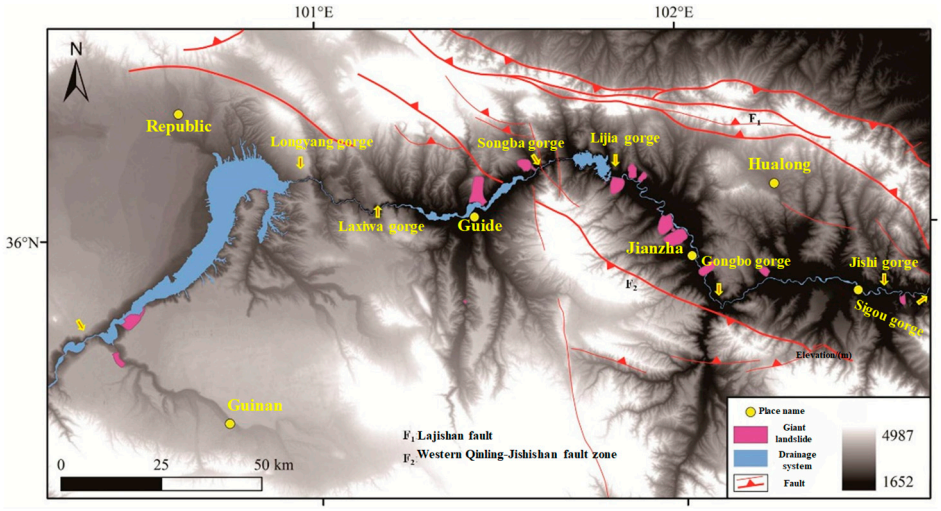

Figure 9. Distribution map of DEM, active structure and giant landslide in the study area.

A detailed field investigation was conducted on the 21 giant landslides, such as the Xiazangtan landslide, Baicetan landslide, Shenguotan landslide, mudflat landslide, and so on. It is considered that the spatial distribution of these giant landslides is very uneven in each basin, each section, and both sides of the main stream. The number of landslides in the cluster-Jianza basin is the largest, with 9 landslides, the largest residual square, and the highest density intensity. Followed by Xunhua Basin 3, Jishi Gorge area 3, Gonghe basin 3, Guide basin 2, and Guanting basin 1.

Table 7. Statistical table of giant landslides in the upper reaches of the Yellow River.

Distribution	Landslide Number	Landslide Name	Longitude	Latitude	Relative Height Difference between Landslide Front and Back Edge	Residual Volume/ $\times 10^8$ m^3	Slope Gradient/°
Gonghe basin	HP1	Landslide on the left bank of Mangla River	100°26′18″	35°43′56″	418	1.20	42
	HP2	White Thorn Beach landslide	100°30′07″	35°49′11″	538	2.84	40
	HP3	Chana landslide	100°48′49″	36°05′38″	350	1.27	35
Guide basin	HP4	Ashgon landslide	101°34′01″	36°09′07″	556	1.60	40
	HP5	Xijitan slippery landslide	101°27′06″	36°03′44″	240	8.40	30
Qunko-jianzha Basin	HP6	Tangse village landslide	101°48′55″	36°05′27″	790	1.20	35
	HP7	Quhe beach mouth landslide	101°56′12″	36°00′28″	700	0.17	51
	HP8	Kangyang landslide	101°57′20″	36°00′05″	715	10.60	42
	HP9	Xiazang Beach landslide	101°58′51″	36°08′51″	300	15.05	30
	HP10	Branch and east landslide	102°03′45″	35°54′36″	608	0.10	20
	HP11	Shenguo Beach landslide	101°53′12″	36°06′32″	730	0.48	30
	HP12	Xia Qiong Temple landslide	101°53′46″	36°06′04″	300	0.35	30
	HP13	Mud flat landslide	101°58′58″	35°59′55″	372	0.86	20
	HP14	Locked slide	102°03′41″	35°54′40″	250	13.55	48
Recirculating basin	HP15	Root landslide	102°32′53″	35°46′43″	400	1.08	25
	HP16	Chaligang landslide	102°21′12″	35°53′57″	500	0.39	25
	HP17	Tangjiacatan landslide	102°14′20″	35°14′20″	305	2.40	30

Table 7. *Cont.*

Distribution	Landslide Number	Landslide Name	Longitude	Latitude	Relative Height Difference between Landslide Front and Back Edge	Residual Volume/ $\times 10^8$ m^3	Slope Gradient/°
Jishi Gorge area	HP18	Mengda Township landslide	102°38′19″	35°49′48″	250	0.16	18
	HP19	Ma Po Dong landslide	102°35′18″	36°49′31″	350	0.42	50
	HP20	Goromb landslide	102°36′45″	35°49′46″	875	1.19	51
Guanting basin	HP21	Badashan landslide	102°55′03″	35°22′05″	350	0.66	35

Field investigation and remote sensing image analysis show that the width of the front and back edges of the giant landslide in the study area and the length and width of the slide body are similar. The relative elevation difference between the top of the back edge of landslide deposits and the shear outlet of the leading edge has three peaks, which are located at 350 m, 550 m, and 750 m, respectively, and the maximum can reach 875 m. This is basically consistent with the results of the relative height difference between high and steep slopes in the basins on both sides of the main stream of the Yellow River. The back wall of most landslides is well preserved, and the slope of the landslide is mostly between 25° and 40°. For example, the average slope of the Xiazangtan landslide located in the Qunke-Jianzha Basin is 26.4°. During the sliding process of the landslide, the front topography reversed, and the water in the middle of the landslide formed a landslide lake with a depth of 26.4 m.

The distribution of landslides in the Sigouxia and Laganxia sections of the upper reaches of the Yellow River is affected and restricted by environmental factors such as landform, stratigraphic lithology, active structure, and climate change. Through remote sensing images and field investigation, it was found that the landslides in the study area are mainly distributed in Qunke-Jianzha Basin, accounting for 29.3% of the total investigated, followed by Xinhua Basin, Gonghe Basin, Guanting Basin, Guide Basin, Laxiwa Gorge, Lijia Gorge, Jishi Gorge, and Gongbo Gorge. The south bank of the Yellow River has more landslides than the north bank. For example, the Guide Basin and Qunke-Jianzha Basin on the south bank have extremely large-scale and high-intensity development, while the north bank has relatively few landslides. The spatial distribution characteristics of landslides are closely related to the factors of landform, active structure, and climate change in the study area. In the process of landslide formation and development, one or several factors may play the main controlling role.

From the analysis of the age of landslide development, ancient landslides and old landslides are the most developed landslides in the study area, and the slide distance is relatively long, belonging to the high-speed remote landslide type. Some landslide slopes once blocked the Yellow River, leaving a large number of landslide remnants on the other side of the Yellow River. For example, the Golongbu landslide (semi-consolidated rock landslide) in the Jishi Gorge area, the Suozi landslide (bedrock landslide), and the Xiazangtan landslide (mudstone landslide) in the Qunke-Jianzha basin.

The spatial distribution patterns of giant landslides in the study area mainly have the following characteristics:

① Giant landslides are mainly distributed in the area bounded by the Jishishan fault and the Laji Mountain fault in the West Qinling Mountains (Figure 9), and the Jianzha

basin is the most developed, accounting for about 1/3 of the total number, showing a concentrated distribution in the region. The topography of the upper reaches of the Yellow River is generally presented as a Neogene red bed basin bounded by the Jishi Mountain and the Lagi Mountain bedrock belt. The Yellow River runs through the basin and forms a deep valley. The phased uplift of the Tibetan Plateau causes the Yellow River to be sharply cut down in stages, and multistage terraces are formed along the valley [27].

② Restricted by river-side erosion, giant landslides in the study area mainly occur at the concave bank and bend of the Yellow River. For example, the mudflat landslide in the Qunke-Jianzha Basin, the Kangdong landslide, and the Golongbu landslide in the Jishi Gorge area all occur at the concave bank of the Yellow River. Meanwhile, landslides occurring at the bend of the river make it easy to block the Yellow River and form barrier lakes. On the other hand, after the occurrence of a landslide, the accumulation body changes the channel and accumulates in the convex bank.

③ The elevation of the giant landslide front is closely related to the terrace. Ac-cording to the distribution of the front elevation of 21 giant landslides, they are concentrated at an elevation of 2000–2200 m. Since the slope foot is the most concentrated part of shear stress, the front elevation of large landslides is usually located near the riverbed elevation [28].

5. Discussion

From the above 4 sections, it can be seen that the cluster of giant landslides in the study area is widely distributed, and analyzing the inducing factors of giant landslides will help guide the prevention and control of giant landslides. This paper discusses the induced factors of giant landslides from the Yellow River erosion effect, historical earthquakes, and modern human engineering activities, taking the Xichengtan giant landslide as an example. The Xichengtan giant landslide is located in the transitional zone between the mountainous area and the river valley on the north coast of the Yellow River in the central part of the Guide Basin and east of the Nongchun River, a first-class tributary of the Yellow River. The terrain at the back edge is high and steep, with a maximum elevation of 3150 m, while the front edge extends to the bank of the Yellow River, with an elevation of about 2220 m and a relative difference in elevation of more than 900 m. The lithology of the basement strata in the landslide area is mainly Proterozoic and Triassic strata, overlying the Xining Group of Paleogene purple sandy conglomerate, sandstone, and silty mudstone. Above the Xining Group, a set of Guide Formation, Quaternary Republican Formation, and Residual Slope Formation with a total thickness of more than 1000 m, dominated by sandstones, conglomerates, and mudstones is unconformably overlain [29–31]. The strata exposed in the landslide area are the Pliocene Guide Formation and the Holocene Floodplain (Figure 10). The slide bed is mudstone, sandstone, and marl of the Pliocene Guide Formation, which is in the form of a layer structure, with a thickness of 0.3–0.5 m in a single layer, weathering is serious, and the yield is 358°∠3°.

During the uplift of the Tibetan Plateau, the northern side of the Yellow River in the Guide Basin has a steeper slope than the southern side due to the differential up-lift of the northern and southern sides of the basin [32]. The Yellow River channel is close to the north side of the mountain in the basin (Figure 11). The Yellow River has a strong lateral erosion effect on the north side of the mountain, so it is easy to form a high and steep slope on the left bank, which has the free-face condition for landslide development. The stratigraphy of the Neoproterozoic Guide Formation on the north bank consists of sandstones, mudstones, and marl, which are prone to destabilizing the strata under the stripping effect of the Yellow River, resulting in a sit-down slide. The study shows that in the early Holocene, the rapid warming of the Tibetan Plateau and ice and snow meltwater led to an increase in the amount of water coming from the upper reaches of the Yellow River, the hydrodynamic energy increased significantly, and the erosion effect on the north bank was enhanced. The early Holocene was also a period of concentrated development of landslides in the upper reaches of the Yellow River in the Lagan Gorge-Shi Gou section [33].

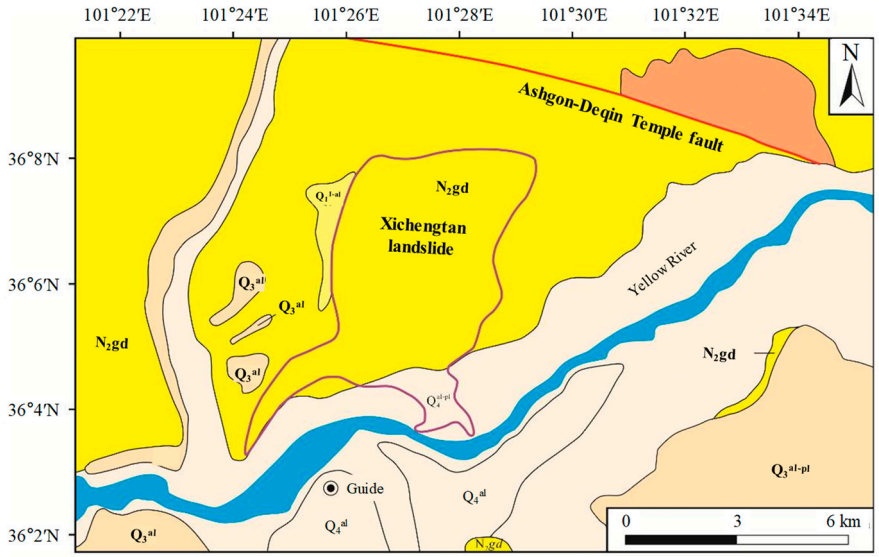

Figure 10. Geological map of the Hitchcock Giant Landslide and adjacent areas.

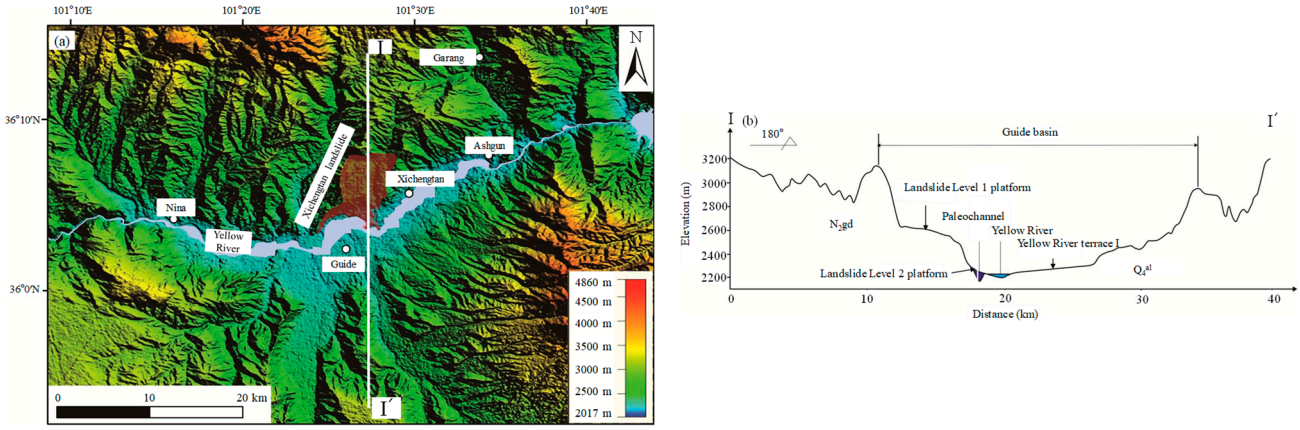

(**a**) (**b**)

Figure 11. The Yellow River channel is close to the north side of the mountain in the basin. (**a**) Topographic map of the Guide Basin; (**b**) Topographic profile across the Yellow River.

Since 1709 A.D., the study area has entered a period of frequent earthquakes and other natural hazards, and earthquakes have been occurring continuously within the Guide earthquake under the influence of the Ashigang-Dechenji active rupture, which has been strongly active since the Holocene [34]. In particular, the 1872 A.D. Guide earthquake caused the dust raised by landslides in the Beishan area of Guide to cover the sky. Therefore, earthquakes are often capable of triggering mega-giant landslides, such as the Daguangbao giant landslide triggered by the Wenchuan earthquake of 12 May 2008 [35] and the Baozi village landslide triggered by the Minxian earthquake of 2013 [36].

In recent decades, droughts and floods have varied greatly in the basin, with annual precipitation essentially concentrated in a short period of 2–3 months, and short periods of sustained precipitation have caused atmospheric precipitation and groundwater to be active along the fracture surfaces and fissure surfaces, which reduces the shear strength of the rock strata and results in the formation of weak structural surfaces [37]. With the intensification of human engineering activities, plazas and viewing platforms have been constructed in the flat area at the leading edge of the landslide in Xichengtan, and these engineering activities have acted as a trailing edge loading on the landslide, which will be an important trigger for the occurrence of the landslide.

6. Conclusions

Based on the study of the spatial plane morphology, distribution characteristics, and spatio-temporal distribution of landslides in the upper reaches of the Yellow River, we have the following three understandings:

(1) Landslide remote sensing images in the upper reaches of the Yellow River have obvious features. The spatial distribution patterns of landslides mainly include dumb-bell shape, rectangle, saddle type, long-arc shape, triangle, and side-by-side shape.

(2) The length and width of the landslide deposit body are mainly concentrated in 550–1500 m and 600–1500 m, and the length and width extend in the direction of polarization. The average elevation of the sliding body is mainly concentrated in the range of 2000–2800 m, and the relative elevation difference between the front and rear edges is concentrated in the vicinity of 150–400 m and 750 m. The average slope of the slide body is mainly distributed in the range of 15–20°.

(3) Giant landslides are mainly distributed in the Jianzha basin area, bounded by the Jishishan fault and the Lashishan fault in the West Qinling Mountains. The giant ancient landslides are mostly multi-stage and distributed in the form of landslide groups.

Author Contributions: Conceptualization, Y.S.; methodology, X.Z.; software, Z.L. and D.L.; validation, R.X.; formal analysis, K.W.; data curation, S.W.; writing—original draft preparation, Z.L.; writing—review and editing, S.W. and P.G.; supervision, K.W.; funding acquisition, Z.L. All authors have read and agreed to the published version of the manuscript.

Funding: This research was funded by the Qinghai Provincial Bureau of Geology and Mineral Exploration and Development Plan Project (2024-24-4) and the Qinghai Key R & D and Transformation Plan Project (2019-SF-130).

Institutional Review Board Statement: Not applicable.

Informed Consent Statement: Not applicable.

Data Availability Statement: Data are contained within the article.

Conflicts of Interest: Author Kai Wu was employed by the company Hubei Shenlong Geological Engineering Investigation Institute Co., Ltd. The remaining authors declare that the research was conducted in the absence of any commercial or financial relationships that could be construed as a potential conflict of interest.

References

1. Huang, R.Q. Large-scale landslides and their sliding mechanisms in china since the 20th century. *Chin. J. Rock Mech. Eng.* **2007**, *26*, 433–445.
2. Wei, Z.X.; Ma, W.L.; Xiao, J.B.; Yin, Z.Q.; Wei, G. Study on the large-scale landslide dammed lake of Songba gorge and its geomorphological effect of the upper reaches of Yellow River. *Chin. J. Geol. Hazard Control* **2017**, *28*, 16–23.
3. Tian, J.J.; Li, T.T.; Pei, X.J.; Ding, F.; Sun, H.; Xie, X.G.; Guo, J. Formation and reactivation mechanisms of large-scale ancient landslides in the Longwu River basin in the northeast Tibetan Plateau, China. *J. Mt. Sci.-Engl.* **2022**, *19*, 1558–1575. [CrossRef]
4. Jia, W.J.; Wang, M.F.; Zhou, C.H.; Yang, Q.H. Analysis of the spatial association of geographical detector-based landslides and environmental factors in the southeastern Tibetan Plateau, China. *PLoS ONE* **2021**, *16*, 0251776. [CrossRef]
5. Yin, Z.Q.; Zhao, W.J.; Qin, X.G. Distribution characteristics of geohazards induced by the Lushan Earthquake and their comparisons with the Wenchuan Earthquake. *J. Earth. Sci.* **2014**, *25*, 912–923. [CrossRef]
6. Terhorst, B.; Kreja, R. Slope stability modelling with SINMAP in a settlement area of the Swabian Alb. *Landslides* **2009**, *6*, 309–319. [CrossRef]
7. Korup, O. Geomorphometric characteristics of New Zealand landslide dams. *Eng. Geol.* **2004**, *73*, 13–35. [CrossRef]
8. Journault, J.; Macciotta, R.; Hendry, M.T.; Charbonneau, F.; Huntley, D.; Bobrowsky, P.T. Measuring displacements of the Thompson River valley landslides, south of Ashcroft, BC, Canada, using satellite InSAR. *Landslides* **2018**, *15*, 621–636. [CrossRef]
9. Li, C.D.; Robert, E.C.; Fu, Z.Y.; Long, J.J.; Tan, Q.W. Evolution characteristics and displacement forecasting model of landslides with stair-step sliding surface along the Xiangxi River, three Gorges Reservoir region, China. *Eng. Geol.* **2021**, *283*, 105961. [CrossRef]
10. Regmi, N.R.; Giardino, J.R.; Vitek, J.D. Characteristics of landslides in western Colorado, USA. *Landslides* **2014**, *11*, 589–603. [CrossRef]
11. Chen, G.J.; Li, C.G.; Chen, S.; Shao, L. Landslide development and the geological process of watercourse evolution in the Three Gorges Reservoir area. *J. Earth. Sci.* **2013**, *38*, 411–416.

12. Yin, Z.Q.; Qin, X.G.; Zhao, W.J.; Gang, W. Characteristics of landslides in upper reaches of yellow river with multiple data of remote sensing. *J. Eng. Geol.* **2013**, *21*, 779–787.
13. Su, H.; Wang, J.P.; Pan, B.T.; Ming, Q.Z.; Shi, Z.T. Sequences and genesis of the Yellow River terraces from Sanmen Gorge to Kouma. *J. Geog. Sci.* **2009**, *34*, 68–72. [CrossRef]
14. Li, J.J.; Fang, X.M.; Ma, H.Z. Geomorphic evolution of upper Yellow River and uplift of Tibetan Plateau in late Cenozoic. *Sci. Sin. (Terrae)* **1996**, *26*, 316–322.
15. Liu, B.C.; Liu, X.F.; Yuan, D.Y.; Zheng, W.X.; Guo, H.; Cao, J.J. Quaternary tectonic activity in northeastern Qinghai-Xizang plateau as reflected by river terraces along the middle-upperreach of the Rellow River. *Seismol. Geol.* **2003**, *25*, 133–145.
16. Guo, Z.Z.; Tian, B.X.; Li, G.M.; Huang, D.; Zeng, T.R.; He, J.; Song, D.Q. Landslide susceptibility mapping in the Loess Plateau of northwest China using three data-driven techniques-a case study from middle Yellow River catchment. *Front. Earth Sci.* **2023**, *10*, 1033085. [CrossRef]
17. Guo, X.H.; Lai, Z.P.; Lu, Y.D.; Li, X.L.; Sun, Z. Optically Stimulated Luminescence (OSL) Chronology of the Dehenglong Landslide from Longyang Gorge to Liujia Gorge along Upper Yellow River, China. *Acta Geol. Sin. Engl.* **2015**, *89*, 242–250.
18. Li, Y.; Meng, H.; Dong, Y.; Hu, S.E. Main Types and characterisitics of geo-hazard in China -Based on the resultsof geo-hazard survey in 290 counties. *Chin. J. Geol. Hazard Control* **2004**, *2*, 29–34.
19. Gariano, S.L.; Guzzetti, F. Landslides in a changing climate. *Earth-Sci. Rev.* **2016**, *162*, 227–252. [CrossRef]
20. Chigira, M. Geologic factors contributing to landslide generation in a pyroclastic area: August 1998 Nishigo Village, Japan. *Geomorphology* **2002**, *46*, 117–128. [CrossRef]
21. Tong, L.Q.; Guo, Z.C. A study of remote sensing image features of typical landslides. *Remote Sens. Nat. Resour.* **2013**, *25*, 86–92.
22. Huang, H.P. *Scale Issues in Object-Oriented Image Analysis*; Institute of Remote Sensing Applications, Chinese Academy of Sciences: Beijing, China, 2003.
23. Drăguţ, L.; Csillik, O.; Eisank, C.; Tiede, D. Automated parameterisation for multi-scale image segmentation on multiple layers. *ISPRS J. Photogramm.* **2014**, *88*, 119–127. [CrossRef] [PubMed]
24. Drăguţ, L.; Tiede, D.; Levick, S.R. ESP: A tool to estimate scale parameter for multiresolution image segmentation of remotely sensed data. *Int. J. Geogr. Inf. Sci.* **2010**, *24*, 859–871. [CrossRef]
25. Zhang, M.; Yin, Y.P.; Wu, S.R.; Zhang, Y.S. Development status and prospects of studies on kinematics of long runout rock avalanches. *J. Eng. Geol.* **2010**, *18*, 805–813.
26. *DZ/T 0261-2014*; Specification of Comprehensive Survey for Landslide, Collapse and Debris Flow (1:50,000). China Geological Survey, China Geological Environmental Monitoring Institute: Beijing, China, 2008; pp. 6–9.
27. Li, X.L.; Guo, X.H.; Li, W.H. Mechanism of giant landslides from Longyangxia valley to Liujiaxia valley along upper Yellow River. *J. Eng. Geol.* **2011**, *19*, 14.
28. Chen, J.; Li, X.; Yang, Z.F. Discussion on the spatiotemporal distribution characteristics and genesis of landslides in the Three Gorges Reservoir Area. *J. Eng. Geol.* **2005**, *13*, 305–309.
29. Liu, S.F.; Zhang, G.W.; Heller, P.L. Cenozoic basin development in the Changhua-Guide region and its indication of plateau accretion. *Sci. China* **2007**, *37*, 235–248.
30. Song, C.H.; Fang, X.M.; Li, J.J.; Gao, J.P.; Sun, D.; Nie, J.S.; Yan, M.D. Late Cenozoic sedimentary evolution and uplift of the northern Tibetan Plateau in the Guide Basin, Qinghai. *Geol. Rev.* **2003**, *49*, 337–346.
31. Liu, S.F.; Zhang, G.W.; Pan, F.; Zhang, H.P.; Wang, P.; Wang, K.; Wang, Y. Timing of Xunhua and Guide basin development and growth of the northeastern Tibetan Plateau, China. *Basin. Res.* **2013**, *25*, 74–96. [CrossRef]
32. Li, X.L.; Ma, J.Q.; Hu, G.S. Analysis of the causes of mega landslides in the Longyangxia-Lujiaxia river section. *Chin. J. Geol. Hazards Prev.* **2007**, *18*, 28–32.
33. Yin, Z.Q.; Wei, G.; Qi, X.B.; Zhou, C.Q. Spatial and temporal characteristics of landslides and there response to climatic change from sigou to lagan gorges in upper reaches of yellow river. *J. Eng. Geol.* **2013**, *21*, 129–137.
34. Hou, G.L.; Yu, C.S.; Xu, C.J. Natural hazards and LUCC and climate change during the historical period in eastern Qinghai. *Arid Zone Resour. Environ.* **2009**, *23*, 86–92.
35. Yin, Y.P.; Zheng, W.M.; Li, X.C.; Sun, P.; Li, B. Catastrophic landslides associated with the Ms 8.0 Wenchuan earthquake. *B. Eng. Geol. Environ.* **2011**, *70*, 15–32. [CrossRef]
36. Yin, Z.Q.; Xu, Y.Q.; Chen, H.Q.; Zhang, Y.J.; Zhao, W.J. Study on the distribution characteristics of geohazards and the causative tectonic of the Minxian-Zhangxian MS6.6 Earthquake on 22 July, 2013, Gansu, China. *Quat. Res.* **2015**, *35*, 88–99.
37. Li, J.H.; Wu, J.; Zhao, J.Z. Characterisation of drought and flood hazard changes in Guide County in the past 50 years. *Soil Water Conserv. Res.* **2012**, *19*, 256–264.